The network connectedness of volatility spillovers across global futures markets

Sang Hoon Kang[a,*], Jang Woo Lee[a]

[a] *Graduate School of Finance, Pusan National University, Busan, Korea*

E-mail: sanghoonkang@pusan.ac.kr

E-mail: jangwoon@pusan.ac.kr

Abstract

This paper analyses the dynamic volatility spillovers and network connectedness between index and commodity futures markets using the multivariate DECO-FIGARCH model and the spillover index method of Diebold and Yilmaz (2014). We estimate a positive equicorrelation between the index and commodity futures and find the highest level of spillover index during the 2008-2009 global financial crisis and 2010-2012 European sovereign debt crisis. Further, we adopt both static and dynamic spillover approaches to identify the net spillover transmitter or receiver across global futures markets. We also measure the directional spillover and assess the net pairwise spillover across global futures markets. Finally, our network connectedness provides specific information on the net pairwise connectedness and intensity of connectedness in different sub-periods.

Keywords: Volatility spillover; network connectedness; global futures markets; financial crises

JEL classification codes: G14; G15

* Corresponding author. Graduate School of Finance, Pusan National University, Jangjeon2-Dong, Geumjeong-Gu, Busan 609-735, Republic of Korea. Tel.: +82 515102558; Fax: +82 515813144. E-mail: sanghoonkang@pusan.ac.kr; kang.sanghoon@gmail.com

1. Introduction

The recent financial crises have renewed interest in complex network topology, through market connectedness (Askari et al., 2018; Majapa and Gossel, 2018). In fact, connectedness is a crucial component of risk and risk management, in particular portfolio concentration risk (Diebold and Yilmaz, 2014).[1] In addition, the measurement of network connectedness provides an "early warning system" for possible upcoming crises, and a system to track the progress of extant crises (Yu et al., 2018). Network connectedness visualizes the propagation path of volatility shocks across financial markets (Cimini, 2015; Liu et al., 2017; Zho et al, 2018). Therefore, portfolio investors examine connectedness with the aim of designing strategies for optimal asset allocation, portfolio optimization, downside risk reductions, and hedging strategies (Majdoub and Mansour, 2014; Kang et al., 2017; Mensi, et al., 2017).

Researchers have recently proposed a variety of methodologies to measure the complex network that exists in financial markets (see An et al., 2018; Dastkahan and Gharneh, 2018; Dimitros and Charakopoulos, 2018; Xi and An, 2018). In earlier studies, Eom et al., (2009) used cross-correlations between stock prices and proposed the minimal spanning tree approach to measure network topology across international stock markets. Adrian and Brunnermeier (2010) introduced the conditional value-at-risk (CoVaR) method, which measures the value-at-risk (VaR) of financial institutions conditional on other institutions experiencing financial distress. Billio et al., (2012) applied principal components analysis and pairwise Granger-causality networks to measure systemic risk in the financial industry. Diebold and Yilmaz (2014) used the spillover index approach to measure both system-wide and pairwise connectedness in US financial firms. Most recently, using the Granger-causality

[1] Diebold and Yilmaz (2014) stated that, to minimize portfolio risk, optimal portfolio allocation requires awareness and measurement of connectedness.

network approach, Baumöhl et al. (2018) analyzed the volatility network across international stock markets. Also, Shahzad, et al. (2018) introduced a bivariate cross-quantilogram approach to examine the net transmitters and receivers of spillovers in complex financial networks.

In order to measure the volatility connectedness network, this paper utilizes the spillover index approach of Diebold and Yilmaz (2014) which assess the magnitude and direction of connectedness across financial variables over time, and hence it provides an alternative way to check the decoupling hypothesis (contagion effect) across global futures markets. In recent years, this spillover index approach has been widely used to examine the connectedness network across different assets (Maghyereh, et al., 2016; Zhang, 2017), institutions (Diebold and Yilmaz, 2014; 2016), CDS sectors (Shahzad, et al., 2018) and markets (Greenwood-Nimmo et al., 2016; Fernández-Rodríguez et al., 2016; Shahzad et al., 2017). Nevertheless, a few studies have explored the network connectedness across global futures markets, while accounting for recent financial crises. In this context, this study analyzes the network connectedness to understanding the transmission of risk spillover across global futures markets.

Our study contributes to the literature in several ways. First, this study uses a multivariate equicorrelation (DECO)-Fractionally Integrated GARCH (FIGARCH) model to assess time-varying correlations between global index and commodity futures markets. The model allows us to capture the long memory property in volatility. Second, this study investigates net and directional connectedness within the network topology of the spillover framework. The spillover index approach provides accurate information on the direction and intensity of risk spillover to investors, thus aiding precise asset allocation and investment decisions. Third, we analyze a rolling sample approach to detect the time-varying dynamics of the spillover index and observe how the recent financial crises may have affected the intensity

and direction of volatility spillovers between index and commodity future markets. The rolling sample approach allows us to examine the risk spillovers over time without having to use a cutoff date to create sub-samples. Similarly, possible economic and financial events must be considered when analyzing a financial time series because arbitrarily chosen sub-samples or non-overlapping intervals cannot capture this dynamic. Fourth, we emphasize the connectedness in each market as a measure of how volatility shocks are transmitted across these markets. That is, we provide a visualization of the complex network to understand the net pairwise connectedness across global index and commodity futures markets. From a practical point of view, our network connectedness informs the price discovery and has profound importance to portfolio managers.

The remainder of this study is organized as follows. Section 2 discusses the methodology used in this study. Section 3 describes the data and presents the preliminary analysis. In section 4 we report and discuss the results, while Section 5 provides concluding remarks.

2. Empirical method

2.1. The DECO-FIGARCH model

In this section, we estimate the multivariate DECO model, allowing us to assess the average of the conditional correlations set equal to the average of all correlation pairs (Engle and Kelly, 2012). In the first stage, we estimate the univariate fractionally integrated GARCH (FIGARCH) model and we presume that the index return (r_t) is expressed by an autoregressive moving average (ARMA (1,1)) model as follows:

$$r_t = \mu + \varphi_1 r_{t-1} + \varepsilon_t + \theta_1 \varepsilon_{t-1}, \qquad t \in N \qquad \text{with} \qquad \varepsilon_t = z_t \sqrt{h_t} \quad , \tag{1}$$

where φ_1 is the AR(1) parameter, θ_1 is the MA(1) parameter, z_t are assumed under the Student-t distribution $\left(z_t \sim ST(0,1,v)\right)$, and h_t is the conditional variance. The FIGARCH$(1,d,1)$ model of Baillie et al., (1996) is defined as follows:

$$h_t = \omega + \beta_1(L)h_t + [1-(1-\beta_1 L)^{-1}(1-\phi L)(1-L)^d]\varepsilon_t^2, \quad (2)$$

where, $\omega > 0$, $\phi_1, \beta_1 < 1, 0 \leq d \leq 1$. d is the fractional integration parameter and L is the lag operator. For $0 \leq$ d ≤ 1, the FIGARCH process captures persistence of shocks to conditional volatility. The fractional differencing operator $(1-L)^d$ is defined as:

$$(1-L)^d = \sum_{k=0}^{\infty} \frac{\Gamma(k-d)L^k}{\Gamma(-d)\Gamma(k+1)} \quad (3)$$

In the second stage, the conditional correlation is estimated using the transformed return residual, which is estimated from the univariate FIGARCH $(1,d,1)$ model. The conditional variance-covariance matrix H_t can be written as:

$$H_t = D_t R_t D_t, \quad (4)$$

where P_t denotes the $(n \times n)$ symmetric matrix of dynamic conditional correlation, and $D_t = diag\left(h_{11,t}^{1/2}, \cdots, h_{NN,t}^{1/2}\right)$, $h_{ii,t}$ represents the conditional variances of each return series. The dynamic conditional correlation matrix P_t decomposes to:

$$R_t = (diagQ_t)^{-1/2} Q_t (diagQ_t)^{-1/2}, \quad (5)$$

$$Q_t = (1-\lambda_1-\lambda_2)\bar{Q} + \lambda_1 u_{t-1}u'_{t-1} + \lambda_2 Q_{t-1}, \quad (6)$$

where Q_t defines the covariance matrix of the standardized residuals $u_t = \left(u_{i,t}, \cdots, u_{k,t}\right)$. $\bar{Q} = cov(u_t, u'_t) = E(u_t, u'_t)$ is the $n \times n$ unconditional covariance matrix of u_t, while λ_1 and λ_2 are non-negative scalars, and $\lambda_1 + \lambda_2 < 1$. The framework of the DECO model is derived from the consistent DCC (cDCC) model of Aielli (2013) by the correlation-driving process:

$$Q_t = (1 - \lambda_1 - \lambda_2)\bar{Q} + \lambda_1\left(Q_{t-1}^{*1/2} u_{t-1} u'_{t-1} Q_{t-1}^{*1/2}\right) + \lambda_2 Q_{t-1}, \quad (7)$$

Using the cDCC framework, Engle and Kelly (2012) document that ρ_t is calculated from the off-diagonal elements of conditional correlation matrix Q_t. This model is named the dynamic equicorrelation (DECO). The equicorrelation is specified as (see Mensi et al., 2017):

$$\rho_t^{DECO} = \frac{1}{n(n-1)}(A'_n R_t^{cDCC} A_n - n) = \frac{2}{n(n-1)} \sum_{i=1}^{n-1} \sum_{j=i+1}^{n} \frac{q_{ij,t}}{\sqrt{q_{ii,t} \cdot q_{jj,t}}}, \quad (8)$$

where $q_{i\,j,t} = \rho_t^{DECO} + a_{DECO}\left(u_{i,t-1}u_{j,t-1} - \rho_t^{DECO}\right) + b_{DECO}\left(q_{i\,j,t} - \rho_t^{DECO}\right)$, which is the (i, j) th element of matrix Q_t from the cDCC model. The scalar equicorrelation is used to estimate the conditional correlation matrix:

$$R_t = (1 - \rho_t) I_n + \rho_t A_n, \quad (9)$$

where A_n is the $n \times n$ matrix of ones, and I_n is the n-dimensional identity matrix. This process allows us to generate a single time-varying correlation coefficient in large sets of assets.

2.2. Spillover Index

To analyze directional volatility spillover across global futures markets, we utilize the generalized VAR of the spillover index of Diebold and Yilmaz (2014) as follows:

$$X_t = \sum_{i=1}^{p} \Psi_i X_{t-1} + \varepsilon_t, \quad (10)$$

where X_t is an Nx1 vector of endogenous variables, Ψ_i are $\mathrm{N} \times \mathrm{N}$ autoregressive coefficient matrices, and $\varepsilon_t \sim (0, \Sigma)$ is a vector of error terms with an *i.i.d.* process. The above VAR process can be rewritten as a moving average process:

$$X_t = \sum_{i=1}^{\infty} \mathrm{Z}_i \, \varepsilon_{t-1} \quad , \quad (11)$$

where the N × N coefficient matrixes Z_i are recursively defined as $Z_i = \sum_{k=1}^{P} Z_{i-k}$, with Z_0 being the N × N identity matrix, and $Z_i = 0$ for i < 0. We analyze the generalized version of H-step-ahead forecast-error variance decomposition as follows:

$$c_{ij}^{g}(H) = \frac{\sigma_{jj}^{-1} \sum_{h=0}^{H-1} (e_i' Z_h \Sigma e_j)^2}{\sum_{h=0}^{H-1} (e_i' Z_h \Sigma Z_h' e_j)}, \quad (12)$$

where the term Σ is a non-orthogonalized covariance matrix of errors corresponding to the VAR system. The term σ_{jj} is a vector of standard deviations of the error term for the j^{th} equation and e_i is an $N \times 1$ vector, which has 1 as the i^{th} element and zero as the other elements.

In the connectedness decomposition table, $C_{i \leftarrow j}^{H}$ indicates pairwise directional spillovers from the futures market j to another futures market i as follows:

$$C_{i \leftarrow j}^{H} = c_{ij}^{g}(H), \quad (13)$$

The directional connectedness from all other futures markets to the futures market i are calculated as:

$$C_{i \leftarrow \cdot}^{H} = \sum_{\substack{j=1 \\ j \neq i}}^{N} c_{ij}^{g}(H), \quad (14)$$

Conversely, the directional connectedness to others from j are calculated as:

$$C_{\cdot \leftarrow i}^{H} = \sum_{\substack{i,j=1 \\ j \neq i}}^{N} c_{ij}^{g}(H), \quad (15)$$

We can also define net directional connectedness as:

$$C_{i}^{H} = C_{\cdot \leftarrow i}^{H} - C_{i \leftarrow \cdot}^{H}, \quad (16)$$

Finally, total connectedness (system-wide connectedness) is the ratio of the sum of the "To" ("From") elements of the variance decompositions matrix to the sum of all elements:

$$C^{H} = \frac{1}{N} \sum_{\substack{i,j=1 \\ j \neq i}}^{N} c_{ij}^{g}(H). \quad (17)$$

To build visual network connectedness, we interpret our connectedness table as the adjacency matrix of a weighted directed network (Diebold and Yilmaz, 2014, 2016). The elements of the adjacency matrix are our pairwise directional connectedness, $C_{i\leftarrow j}^{H}$; the row sums of the adjacency matrix (node in-degrees) are our total directional connectedness "From", $C_{i\leftarrow\cdot}^{H}$; and the column sums of the adjacency matrix (node out-degrees) are our total directional connectedness "To", $C_{\cdot\leftarrow i}^{H}$.

3. Data and preliminary analysis

3.1. Data

We use daily price data for twelve equity index futures: iBovespa index futures (BOVESPA) for Brazil, CAC 40 index futures for France, DAX index futures for Germany, the UK FTSE 100 futures index (FTSE 100), Hang Seng index futures (HANGSENG) for Hong Kong, IBEX 35 futures index (IBEX 35) for Spain, the Korean KOSPI 200 index futures (KOSPI 200), NIFTY index futures (NIFTY) of India, Nikkei 225 index futures (NIKKEI 225) for Japan, the US S&P 500 index futures (S&P 500), S&P/ASX index futures (SPI 200) of Australia, and Singapore's Straits Times index futures (Strait Times). We also consider two commodity futures markets, WTI crude oil and gold futures contracts. The study period is January 1, 2002 to July 19, 2018, which covers several turbulent periods and crises, including the 2008–2009 Great Financial Crisis (GFC) and the 2010–2012 European Sovereign Debt Crisis (ESDC). The data for all series are extracted from DataStream.

We calculate continuously compounded daily returns by taking the difference in the logarithm percentage of two consecutive prices. To avoid biases from different trading time across borders (i.e. nonsynchronous trading and short-term correlations from noise), we apply

the average two-day rolling returns to account for different market trading time (Forbes and Rogobon, 2002).

Figure 1 below plots the dynamic two-day average returns of global futures for each of the above futures indices, together with crude oil and gold for the sample period. This figure shows periods of significant fluctuations with all futures returns exhibiting volatility clustering. We apply the Markov-switching-dynamic regression (MS-DR) to detect two tranquil and volatile regimes in the return series that allows one to identify the beginning and the end of each phase of the financial crises, which is of great importance when one deals with the cross-futures market spillovers issue. The shaded regions [Regime 1] show the regimes of excess volatility according to the MS-DR and show the effects of the 2002 dotcom crisis, 2008-2009 GFC, and 2010-2012 ESDC. Comparing the two commodity markets shows that oil is more volatile than gold.

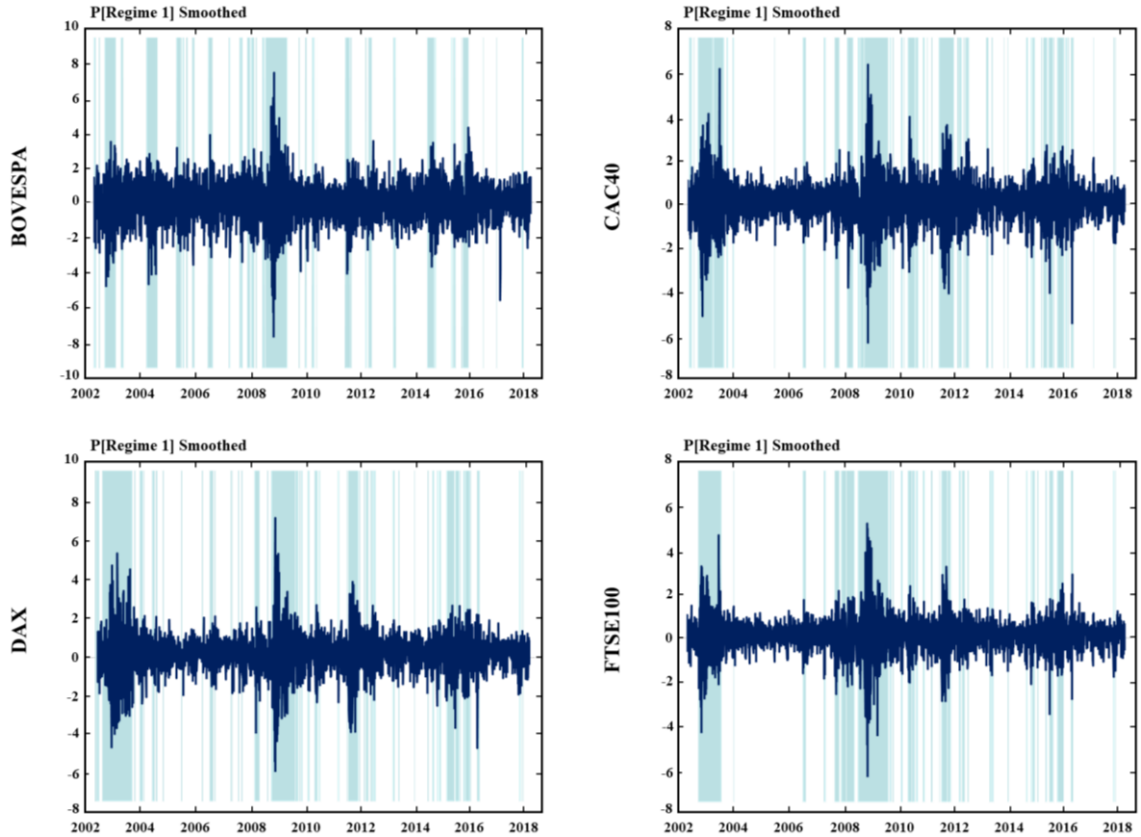

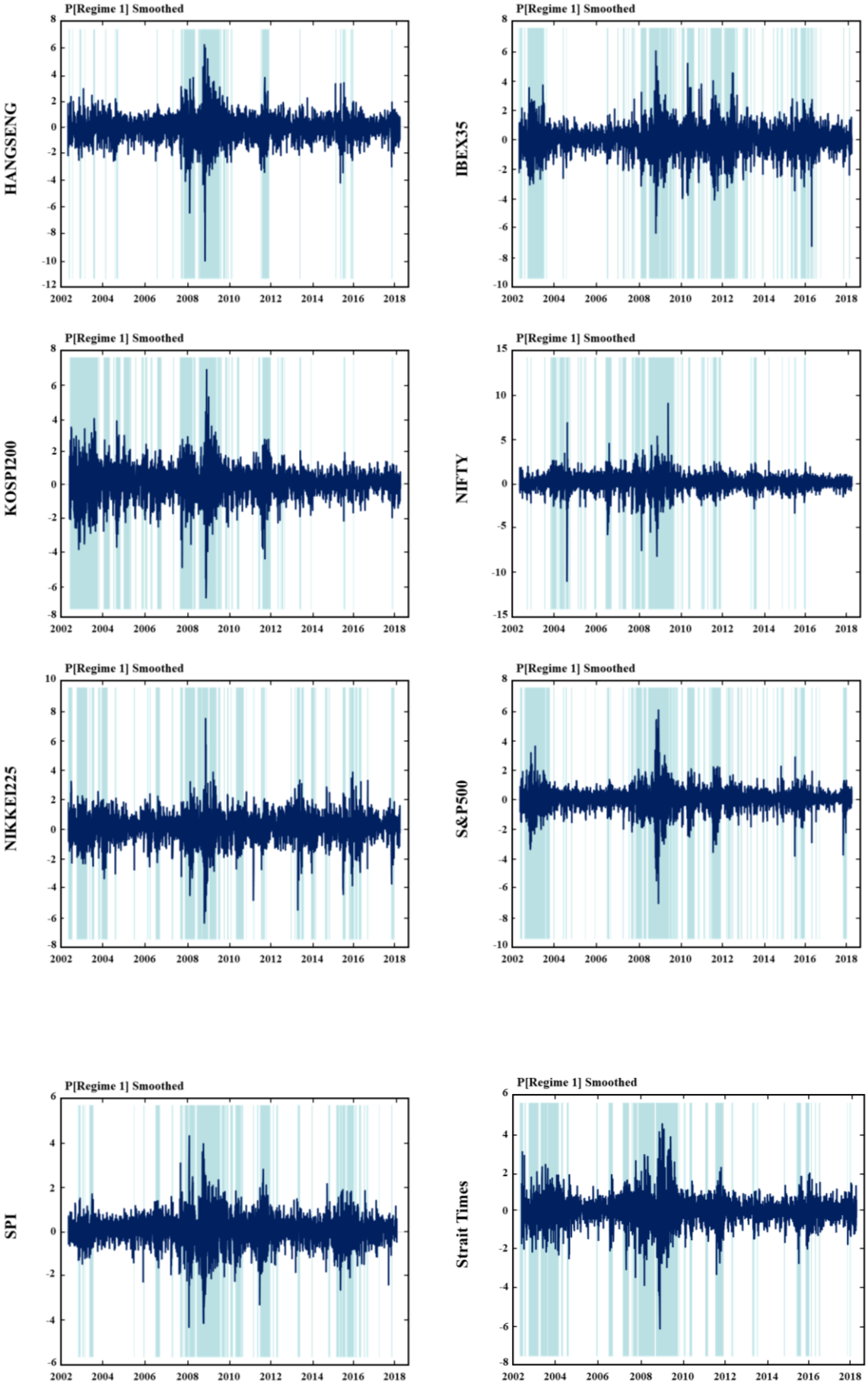
HANGSENG
P[Regime 1] Smoothed
IBEX35
P[Regime 1] Smoothed
KOSPI200
P[Regime 1] Smoothed
NIFTY
P[Regime 1] Smoothed
NIKKEI225
P[Regime 1] Smoothed
S&P500
P[Regime 1] Smoothed
SPI
P[Regime 1] Smoothed
Strait Times
P[Regime 1] Smoothed

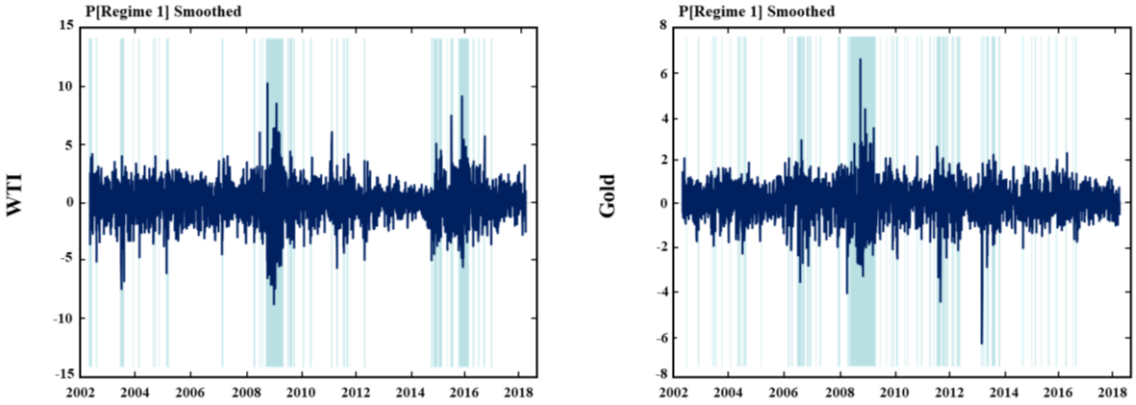

Fig. 1. Dynamics of the global futures market returns

Note: The MS-DR model highlight the excess volatility in the shaded areas [Regime 1].

3.2. Preliminary analysis

Table 1 below provides descriptive statistics of daily futures returns and unit root tests, for the index and commodity futures markets. We can see that NIFTY has the highest average returns for the sample period. The standard deviation is the highest for WTI oil futures, indicating the highest risk among all futures markets. All skewness coefficients are negative and the kurtosis coefficients are higher than three for all return series, indicating that the probability distributions of the futures returns are skewed and leptokurtic, supporting non-normality; this is confirmed by Jarque-Bera statistics. According to the ADF unit root statistics test, and the stationarity test of the KPSS test results, all return series are stationary. Further, the Ljung-Box Q(30) and Q^2(30) tests for serial correlation of residuals and square residuals, respectively, as well as the ARCH effect in the return series by applying the ARCH LM(10) tests. The results highlight the presence of both serial correlation and the ARCH effect in all cases. Therefore, we apply a FIGARCH model to capture some stylized facts, such as fat-tails, clustering volatility and persistence for index and commodity futures returns.

Fig. 2 displays the heat map of Pearson's correlation matrix among global futures markets. Note that the color indicates the strength of the correlation, from blue (positive) to red (negative). As shown in Fig. 2, the global futures returns have a significantly strong and positive correlation, indicating the connectedness among global futures markets. In particular, the Eurozone futures markets (IBEX35, FTSE 100, CAC 40, DAX) are significantly related to one another. For commodity futures markets, gold is negatively and weakly correlated with other futures markets, implying that gold futures as a refuge asset provide a possible diversification benefit for investors.

Table 1. Descriptive statistics of global equity and commodity futures markets

	Mean(%)	Max.	Min.	Std. dev.	Skewness	Excess Kurtosis	Jarque-Bera	Q(30)	$Q^2(30)$	ADF	KPSS	ARCH-LM(10)
BOVESPA	0.00276	7.8723	-8.0414	1.1978	-0.2612	2.7813	1434.6***	556.9***	8272.***	-31.19***	0.0866	182.37***
CAC40	0.00365	6.7124	-6.7216	0.9805	-0.1993	4.4685	3605.1***	432.0***	7116.***	-31.28***	0.1082	135.02***
DAX	0.01714	7.4452	-6.3284	1.0063	-0.3172	4.3954	3532.7***	438.9***	8131.***	-29.78***	0.1636	157.62***
FTSE100	0.00880	5.4437	-6.7481	0.7997	-0.2903	6.6569	7998.2***	398.0***	8988.***	-30.56***	0.0634	181.93***
HANGSENG	0.02969	6.6695	-10.519	0.9952	-0.3874	6.8982	8631.3***	432.4***	6052.***	-30.58***	0.0364	155.54***
IBEX35	0.01291	6.3624	-7.5929	1.018	-0.2593	4.1127	3078.0***	431.3***	4820.***	-31.23***	0.0486	133.18***
KOSPI200	0.02801	7.2308	-7.2553	0.9849	-0.3882	4.5112	3753.4***	449.8***	7162.***	-30.15***	0.1082	204.70***
NIFTY	0.04635	9.5267	-11.67	1.0294	-0.6881	12.185	26934.***	297.0***	1949.***	-29.35***	0.2599	88.634***
NIKKEI225	0.01804	7.7977	-6.8094	0.9871	-0.4075	4.0694	3085.2***	502.7***	4311.***	-29.73***	0.1463	120.22***
S&P500	0.02069	6.3931	-7.3791	0.8028	-0.5541	8.7822	14035.***	300.9***	12281.***	-30.47***	0.2184	256.57***
SPI200	0.02020	4.5405	-4.5688	0.6965	-0.3616	4.3007	3406.8***	491.2***	9059.***	-31.18***	0.0874	194.23***
Strait Times	0.01568	4.7977	-6.4426	0.7637	-0.2467	5.8928	6263.7***	443.8***	6828.***	-29.25***	0.1122	208.44***
WTI	0.02769	10.779	-9.235	1.5879	-0.1626	3.5509	2277.5***	517.0***	5695.***	-28.59***	0.2346	107.66***
Gold	0.03441	6.9042	-6.8776	0.7950	-0.4246	5.2230	5015.6***	455.4***	1829.***	-28.77***	0.2944	84.792***

Notes: The asterisk *** denotes rejection of the null hypotheses of normality, no autocorrelation, unit root, stationarity, and conditional homoscedasticity.

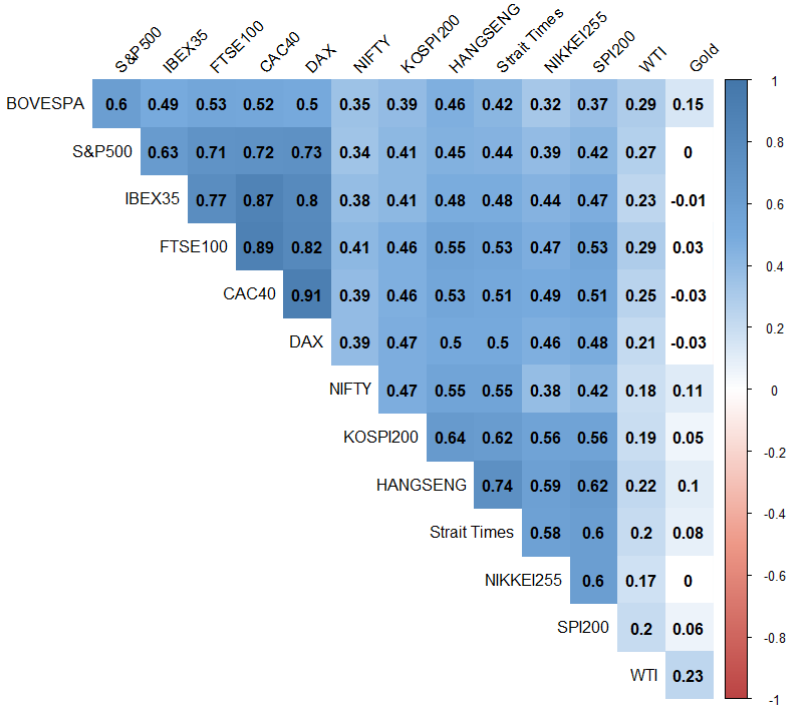

Fig. 2. Heat map of the correlation matrix

Note: This figure shows a visual correlation matrix across global futures markets. The color boxes indicate the strength of the correlation. Blue indicates a positive correlation, while red indicates a negative correlation.

4. Empirical results

4.1 Estimation of DECO-FIGARCH model

Table 2 reports the estimate results of the multivariate DECO-FIGARCH (1, *d*, 1) for global index and commodity futures markets. In Panel A, the moving average parameter is statistically significant at the 1% level for all futures returns. Both ARCH (ϕ_1) and GARCH (β_1) terms are significant. More importantly, the fractional integrated coefficient (d) is significant for all markets, thus revealing the presence of long memory behavior in global futures markets.

In Panel B, the parameter (a_{DECO}) is positive and significant at the 1% level, indicating the importance of shocks across the global futures markets. The parameter (b_{DECO}) is significant and very close to one, confirming the higher persistence of volatility across the global index and commodity futures markets. We also show that the dynamic equicorrelation $(\rho_t^{DECO})$is positive and weak (0.1976), providing the diversification benefits between index and commodity futures. The diagnostic results in the bottom row of Table 2 suggest no serial correlation estimated by Ljung-Box statistics for the squared standardized residuals thus validating our DECO-FIGARCH model.

Table 2. Estimation of multivariate ARMA(1,1)-FIGARCH(1,d,1)-DECO model

	BOVESPA	CAC40	DAX	FTSE 100	HANGSENG	IBEX 35	KOSPI 200	NIFTY	NIKKEI 225	S&P 500	SPI 200	Strait Times	WTI	Gold
Panel A: Estimates of ARMA-FIGARCH(1,d,1) model														
Const. (μ)	0.025	0.055***	0.073***	0.040***	0.059***	0.066***	0.043***	0.064***	0.061***	0.063***	0.047***	0.039***	0.064**	0.028*
	(0.022)	(0.014)	(0.016)	(0.011)	(0.016)	(0.016)	(0.015)	(0.017)	(0.017)	(0.011)	(0.011)	(0.011)	(0.027)	(0.015)
AR(1)	-0.028	-0.029**	-0.001	-0.033**	-0.010	0.003	-0.025*	0.025	-0.019	-0.060***	-0.024	0.003	-0.040**	-0.014
	(0.015)	(0.016)	(0.015)	(0.015)	(0.015)	(0.017)	(0.014)	(0.017)	(0.015)	(0.015)	(0.016)	(0.015)	(0.016)	(0.015)
MA(1)	0.984***	0.979***	0.982***	0.991***	0.986***	0.979***	0.989***	0.983***	0.987***	0.987***	0.989***	0.989***	0.983***	0.986***
	(0.003)	(0.002)	(0.002)	(0.001)	(0.002)	(0.002)	(0.001)	(0.002)	(0.002)	(0.002)	(0.001)	(0.002)	(0.002)	(0.001)
Const. (ω)	0.856***	0.538**	0.642***	0.267***	0.580***	0.533***	1.369***	0.696**	0.988**	0.860*	0.191***	1.047***	2.496**	0.306***
	(0.267)	(0.216)	(0.275)	(0.105)	(0.193)	(0.225)	(0.686)	(0.292)	(0.392)	(0.446)	(0.056)	(0.584)	(1.051)	(0.086)
d-FIGARCH	0.358***	0.496***	0.513***	0.494***	0.456***	0.467***	0.585***	0.525***	0.536***	0.534***	0.460***	0.642***	0.563***	0.409***
	(0.075)	(0.042)	(0.044)	(0.041)	(0.060)	(0.043)	(0.059)	(0.054)	(0.052)	(0.053)	(0.041)	(0.062)	(0.077)	(0.063)
ARCH (ϕ_1)	0.112	0.081	0.080*	0.148***	0.189***	0.110***	0.110***	0.228***	0.179***	0.098	0.290***	0.178***	0.313***	0.345***
	(0.130)	(0.058)	(0.047)	(0.047)	(0.051)	(0.042)	(0.031)	(0.054)	(0.043)	(0.076)	(0.047)	(0.039)	(0.046)	(0.069)
GARCH (β_1)	0.449**	0.512***	0.550***	0.552***	0.624***	0.514***	0.696***	0.680***	0.643***	0.526***	0.650***	0.747***	0.783***	0.708***
	(0.181)	(0.074)	(0.065)	(0.061)	(0.086)	(0.054)	(0.056)	(0.051)	(0.058)	(0.090)	(0.053)	(0.047)	(0.057)	(0.068)
Panel B: Estimates of the DCC model														
ρ_t^{DECO}	0.1976***													
	(0.0432)													
a_{DECO}	0.0140***													
	(0.0032)													
b_{DECO}	0.9857***													
	(0.0033)													
df	7.3539***													
	(0.2288)													
$Q^2(30)$	29.70	32.19	14.86	22.95	43.16	26.76	21.49	25.88	33.20	33.68	29.62	36.80	20.47	31.76
	[0.480]	[0.358]	[0.990]	[0.817]	[0.056]	[0.635]	[0.871]	[0.681]	[0.313]	[0.293]	[0.484]	[0.182]	[0.903]	[0.307]

Notes: The p-values are reported in brackets [.]. The standard error values are reported in parentheses (.). ** and *** indicate significance at the 5% and 1% levels, respectively.

Fig. 3 plots the dynamic equicorrelation between the index and commodity futures markets. As shown in Fig. 3, we observe time-varying correlations over the sample period, suggesting that institutional investors do or should frequently change their portfolio structure. A significant increase in correlation is observed during the two recent crises (2008–2009 GFC and 2010–2012 ESDC), supporting the market contagion among the global futures markets. Between 2013 and 2014, equicorrelation among futures markets decreased, before subsequently rising due to increased uncertainties relating to the 2015 commodity market collapse, Chinese market crash, 2016 Brexit, and the 2018 US Fed interest rate hike. Thus, portfolio investors reconstruct their portfolio structures based on the increase/decrease phases in time-varying correlations during the sample period.

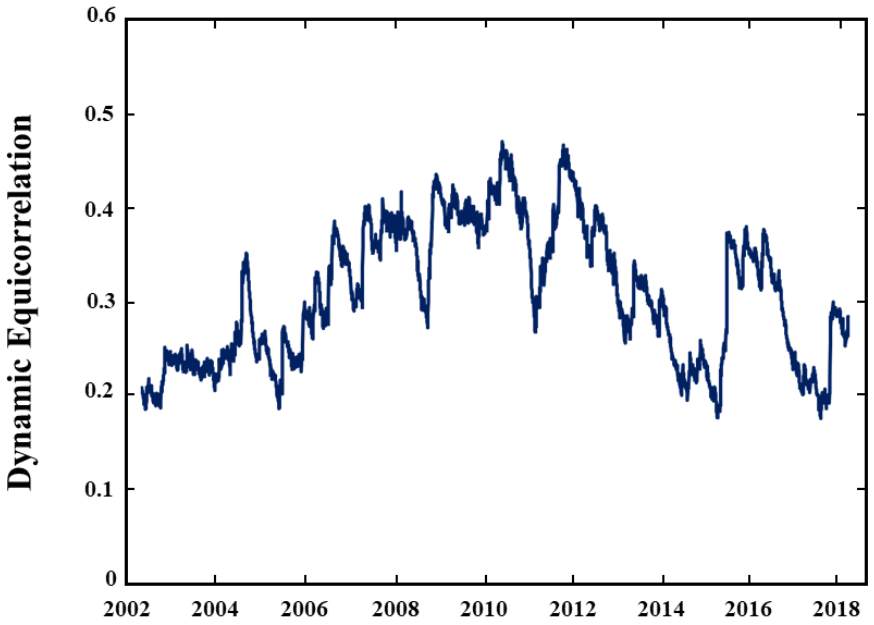

Fig. 3. Dynamic equicorrelation among the global futures markets

4.2 Total volatility spillovers

Tables 3-4 report the estimates of the static volatility spillover matrix. The $(i, j)^{th}$ entry in each panel is the estimated contribution to the forecast-error variance of variable *i*, coming from innovations to market *j*. The row sums, excluding the main diagonal elements (termed "From") and column sums (termed "To"), report the total spillovers to (received by) and from (transmitted by) each volatility.

Table 3 presents the total spillovers across the global index futures markets only. In the lower right corner of Table 3, the total spillover reaches 62.90%, implying a high connectedness across the global index futures markets. Looking at the directional spillovers transmitted 'To,' the FTSE 100 is the largest transmitter to other futures markets, contributing 148.2%, followed by CAC 40 (130.1%) and the S&P 500 (96.3%). The results suggest that the UK futures market is the main source of volatility spillover shock to other index futures markets. Notably, the KOSPI 200 index futures market of the Korean Exchange (KRX) contributes only 4% of total volatility spillover to other index futures markets, and it receives a total of 69.2% of its return spillover from other index futures markets. This indicates that the KOSPI 200 index futures market is the largest receiver of volatility spillover from other futures markets.

Table 4 presents total volatility spillovers across index futures markets by adding commodity futures markets (WTI futures and gold futures). The lower right corner in Table 4 reveals that the total spillover reaches 55.6%. Although the overall spillover shock is still high, there is a reduction of total volatility spillover from 62.90%, the total spillover of the index futures markets only in Table 3. The results also show the role of commodity futures markets as refugee index futures markets, consistent with results from previous studies including, among others, Baur and Lucey (2010), Baur and McDermott (2010), and Bredin et al. (2015).

Using a rolling window approach, Fig. 3 plots the time-varying total volatility spillover index of the index futures markets, adding commodity futures markets. Fig. 3 highlights significant variation in the volatility spillover index, which is shown to be very responsive to the various financial and economic events. It can be seen that the total volatility spillovers attain their maximum level during 2008–2009 and 2010-2012, corresponding to the GFC and two ESDC stages. Moreover, (d) the Chinese stock market collapse and commodity market crash in August 2015, and the changes of interest rates by (e) the U.S. Federal Reserve in March 2018, intensify the spillovers among global futures markets, which reduces the diversification opportunities for these markets. Therefore, the economic and financial crises intensify the total spillovers across global futures markets.

Table 3. Total volatility spillovers within equity index futures markets

	BOVESPA	CAC40	DAX	FTSE 100	HANGSENG	IBEX 35	KOSPI 200	NIFTY	NIKKEI 225	S&P 500	SPI200	Strait Times	From
BOVESPA	35.9	9.17	4.93	16.26	1.27	6.02	0.1	1.16	0.52	16.64	1.96	6.06	64.1
CAC40	1.31	27.74	11.71	22.08	1.46	18.28	0.24	0.55	0.56	10.55	1.39	4.13	72.3
DAX	1.39	21.99	23	19.73	1.58	12.7	0.02	0.55	0.73	12.85	0.9	4.55	77
FTSE100	1.39	21.13	9.29	32.93	1.25	10.71	0.44	0.65	0.67	13.98	1.61	5.96	67.1
HANGSENG	3.93	6.06	3.57	9.16	31.72	5.1	0.04	4.09	4.93	6.28	10.99	14.13	68.3
IBEX35	0.78	23.56	7.14	14.41	0.96	39.7	0.26	0.47	0.81	6.29	1.93	3.68	60.3
KOSPI200	5.09	7.39	6.27	8.92	7.86	4.95	30.83	3.31	3.86	10.25	1.74	9.53	69.2
NIFTY	3.47	1.69	0.7	3.44	2.59	2.07	0.33	70.67	0.5	0.75	2.96	10.81	29.3
NIKKEI225	2.81	6.73	2.79	8.24	8	5.31	0.13	1.34	44.56	4.38	6.19	9.52	55.4
S&P500	2.17	12.28	6.67	18.05	1.68	8.37	0.5	0.47	0.91	39.78	2.93	6.19	60.2
SPI200	2.41	10.81	3.43	13.42	4	7.2	2.6	1.65	3.55	7.04	34.17	9.7	65.8
Strait Times	4.43	9.29	3.2	14.48	7.63	5.54	0.19	3.26	3.67	7.27	6.67	34.38	65.6
To	29.2	130.1	59.7	148.2	38.3	86.3	4.9	17.5	20.7	96.3	39.3	84.3	754.6
All	65.1	157.9	82.7	181.1	70	125.9	35.7	88.2	65.3	136.1	73.4	118.6	62.90%
Net	-34.9	57.8	-17.3	81.1	-30	26	-64.3	-11.8	-34.7	36.1	-26.5	18.7	

Notes: The (i,j)th element of the table shows the estimated contribution to the variance of the 10-day-ahead forecast error of *i* from innovations to variable *j*. The diagonal elements (*i*=*j*) are the own variance shares estimates, which indicate the fraction of the forecast error variance of market *i* that is the result of its own shocks.

Table 4. Total volatility spillovers within index and commodity futures markets

	BOVESPA	CAC40	DAX	FTSE 100	HANG SENG	IBEX 35	KOSPI 200	NIFTY	NIKKEI 225	S&P 500	SPI 200	Strait Times	WTI	Gold	From
BOVESPA	35.74	9.01	4.92	15.97	1.27	6.04	0.06	1.13	0.45	16.46	1.76	5.77	1.11	0.31	64.3
CAC40	1.33	27.63	11.84	21.77	1.45	18.44	0.19	0.46	0.54	10.41	1.21	4.01	0.59	0.13	72.4
DAX	1.4	21.87	23.2	19.5	1.57	12.74	0.02	0.49	0.7	12.77	0.79	4.45	0.44	0.03	76.8
FTSE100	1.38	20.89	9.37	32.66	1.24	10.75	0.34	0.55	0.63	13.82	1.38	5.75	1.07	0.19	67.3
HANGSENG	3.96	5.92	3.57	8.91	32.2	5.1	0.02	4	4.9	6.21	10.74	14.01	0.36	0.1	67.8
IBEX35	0.82	23.42	7.15	14.2	0.94	39.76	0.24	0.42	0.81	6.2	1.85	3.65	0.44	0.1	60.2
KOSPI200	5.35	7.39	6.23	9.01	7.76	4.88	29.95	3.21	4.02	10.3	1.85	9.94	0.05	0.07	70
NIFTY	3.69	1.46	0.7	3.08	2.58	1.98	0.38	70.93	0.52	0.66	2.76	10.98	0.05	0.23	29.1
NIKKEI225	2.74	6.62	2.8	8.01	8.12	5.34	0.15	1.28	45.08	4.27	5.93	9.24	0.39	0.03	54.9
S&P500	2.16	12	6.68	17.66	1.67	8.34	0.44	0.41	0.87	39.76	2.71	6.03	0.98	0.3	60.2
SPI200	2.41	10.56	3.46	13.03	4.06	7.26	2.4	1.48	3.53	6.9	34.29	9.53	0.75	0.34	65.7
Strait Times	4.36	9.08	3.23	14.09	7.89	5.64	0.12	3.17	3.54	7.13	6.22	34.59	0.76	0.16	65.4
WTI	0.13	1.61	0.07	4.35	0.38	0.53	0.23	0.04	0.1	0.82	0.37	0.15	88.53	2.69	11.5
Gold	0.58	0.83	0.12	3.13	0.41	0.78	0.2	0.8	0.38	0.51	2.63	0.54	1.88	87.22	12.8
To	30.3	130.7	60.1	152.7	39.3	87.8	4.8	17.4	21	96.4	40.2	84.1	8.9	4.7	778.4
All	66.1	158.3	83.3	185.4	71.5	127.6	34.7	88.4	66.1	136.2	74.5	118.7	97.4	91.9	55.60%
Net	-34	58.3	-16.7	85.4	-28.5	27.6	-65.2	-11.7	-33.9	36.2	-25.5	18.7	-2.6	-8.1	

Notes: See Table 3.

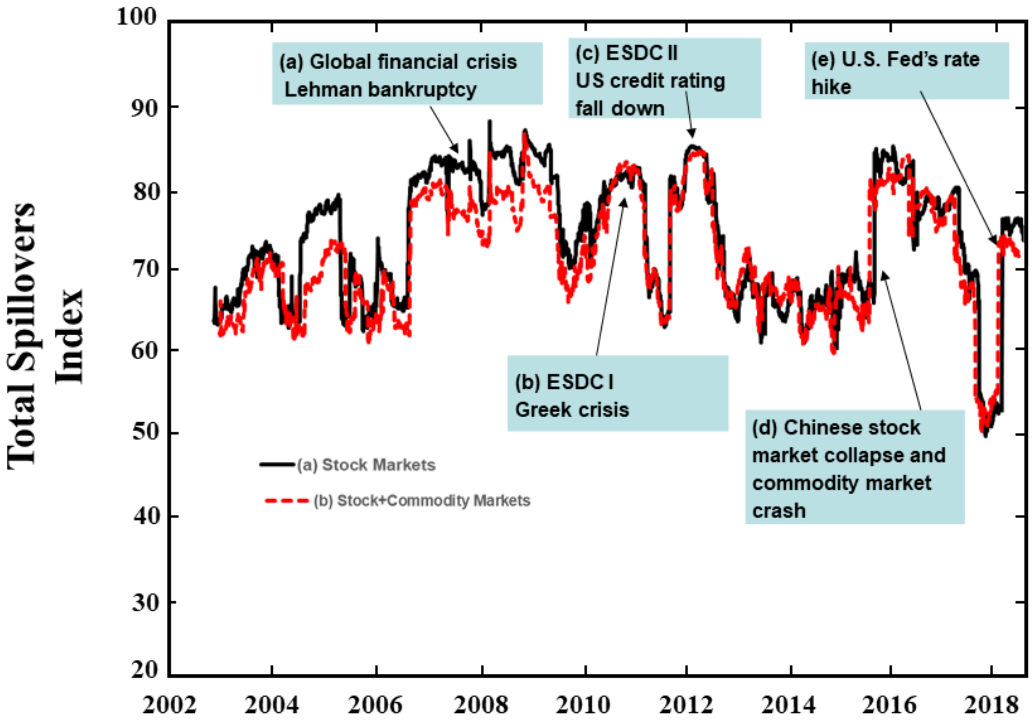

Fig. 3. Dynamics of the volatility spillover index

Notes: The time evolution of spillovers indices is estimated using 200-day rolling windows.

We now discuss the pairwise directional volatility spillover across global futures markets. Fig. 4 shows the system-wide network connectedness of the pairwise direction volatility spillover index based on Table 4. Note that the pairwise spillovers between index futures and commodity futures markets are shown as nodes and edges, respectively, making it a typical complex network. We observe clear clustering between index futures markets, while the two commodity futures markets (gold and WTI) are isolated. In addition, we identify FTSE 100, CAC 40, S&P 500, IBEX 35, and Strait Times (red nodes) as transmitters of volatility shocks, whereas the remaining markets (green nodes) are receivers of shocks of different magnitudes. The graphical evidence is consistent with the results in Table 4.

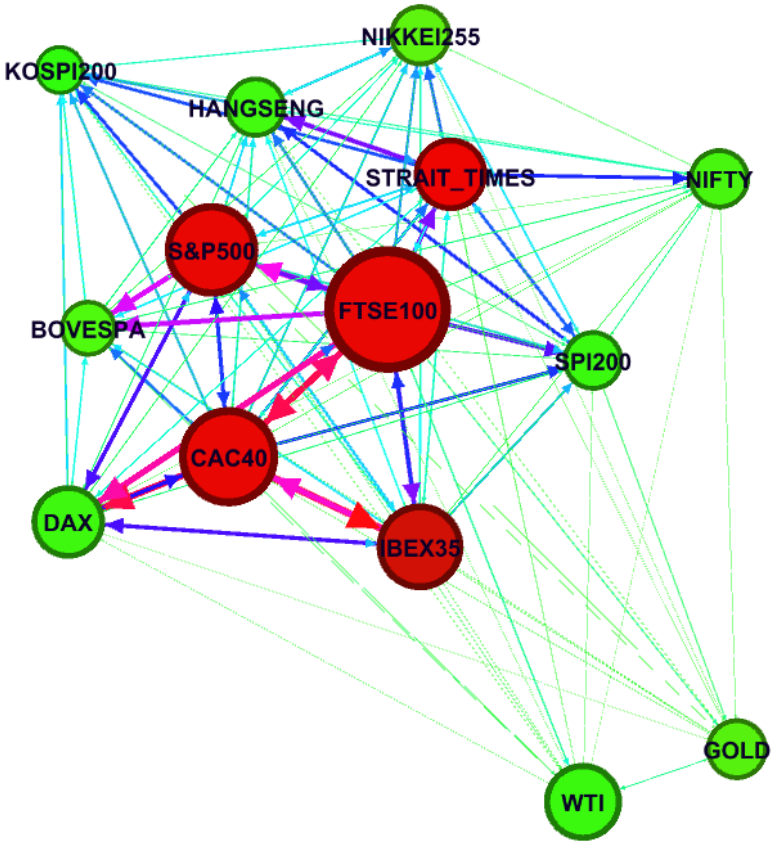

Fig. 4. System-wide network connectedness among the global futures markets

Note: This figure shows system-wide network connectedness among the global futures markets. A node's red (green) color indicates the most significant transmitter (receiver). The edge size indicates the magnitude of the pairwise spillover, whereas the magnitude is also reflected in the color type (green (weak), light blue (medium), or blue and red (strong)).

4.3 Network connectedness

To further explore the dynamic connectedness of risk spillovers, we depict net pairwise network connectedness, which reveal information about risk spillover among the stock-commodity futures markets. Fig. 5(a)-(e) give results for network connectedness of net pairwise directional spillovers, focusing on cases where the intensity was especially significant. The directional spillover network diagram shows the pathway of shocks from one asset class to another, depicted through idiosyncratic shocks. The width of the arrows

indicates the intensity of volatility spillovers and node diameter indicates the size of net spillover. For example, for the first event (November 19, 2008 Global financial crisis in Fig 5(a)), the US futures market is the strongest sender of volatility shocks to gold, and Strait Times of Singapore futures market gives pairwise shocks to Hong Seng of Hong Kong, Nikkei 225 of Japan and SPI 200 of Australia. However, KOSPI 200 (Korea) and Hang Seng (Hong Kong) futures markets are net pairwise receivers of volatility shocks during the global financial crisis. This picture is reasonable because both the Korean and Hong Kong futures markets have the highest foreign (especially US and Europe) ownership ratio among the sample markets.

Network connectedness depicted in Fig 5(b) shows that during the Greek crisis (ESDC I) net pairwise connectedness is more complex. It can be noted that European countries (FTSE 100, IBEX35, CAC40, DAX) become strong or moderate net pairwise transmitters of volatility shocks during the ESDC I. Fig 5(c) illustrates, for the ESDC 2, that SPI 200 futures of Australia is the strongest net pairwise transmitter market of volatility shocks, while KOSPI 200 futures of Korea is the weakest.

Moreover, the US and UK index futures markets dominate network connectedness during the 2015 Chinese and commodity market crashes (in Fig 5(d)). More interestingly, the commodity futures (WTI and gold) markets are net receivers of volatility shocks in the commodity-stock pairwise connectedness. This can be accounted for by the global economic recession leading to lower growth in China and lower demand for commodities. Finally, the US index futures market is the hub market of volatility shocks on 21st March 2018 due to the increase in the US Fed's interest rate, as per Fig 5(e). Overall, it is evident that the direction and magnitude of net volatility spillovers can be difficult to identify and are sensitive to financial and economic events. These results have important implications for portfolio risk assessments.

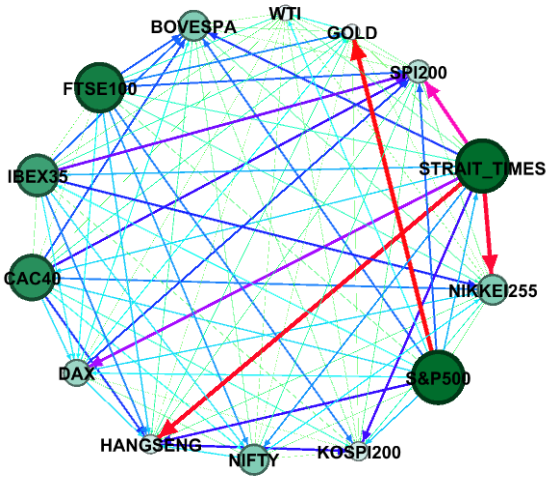

(a) November 19th, 2008
Global financial crisis

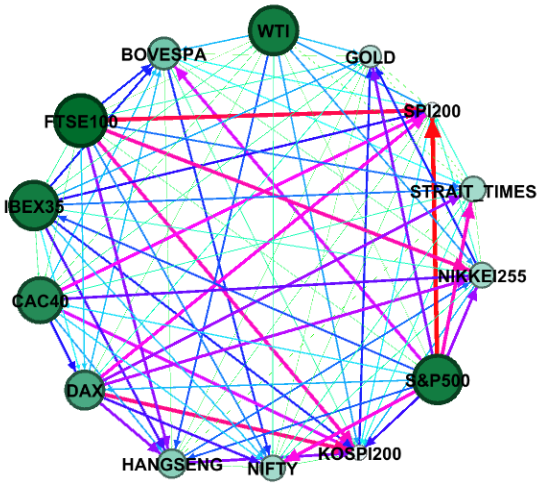

(b) September 10th, 2010
ESDC I Greek crisis

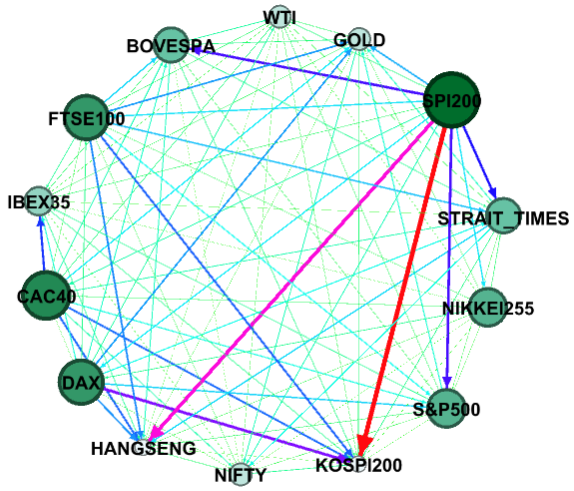

(c) September 9th, 2011
ESDC II U.S. credit rating fall down

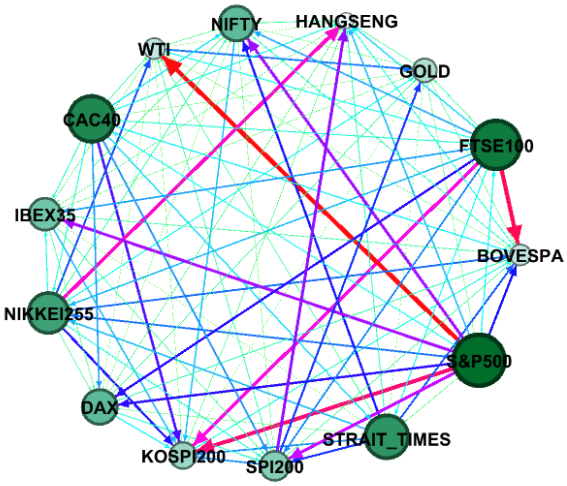

(d) August 31st, 2015
Chinese and commodity markets crashes

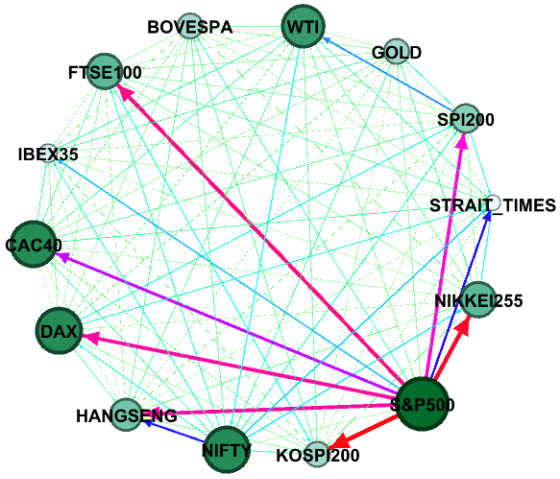

(e) March 21st, 2018
U.S. Fed's rate hike

Fig. 5. Net pairwise directional network during financial and economic events

Note: This figure shows the net pairwise directional connections among the global futures markets. The size of a node indicates the magnitude of a net pairwise connection. The edge size indicates the magnitude of the net pairwise connectedness, and the magnitude is also reflected through the color type (green (weak), light blue (medium), and blue and red (strong)).

5. Conclusions

In this study, we aim to understand dynamic connectedness between global index and commodity futures markets, using both the multivariate DECO-FIGARCH model and the spillover index model of Diebold and Yilmaz (2014). In particular, we analyze the dynamics of directional and net spillovers that reveal the intensity and direction of network connectedness in complex futures markets.

Our empirical results are summarized as follows. First, we observe a significant increase in the dynamic correlations between global futures indices and commodity futures during the recent global financial crisis and European sovereign debt crisis. The increase in correlation in 2008 is found to be related to the historical that time, indicating a contagion effect. Between 2013 and 2014 the correlation between commodity and index futures markets decreased. This result supports the evidence on the decoupling hypothesis and diversification opportunities. The increase/decrease phases in the time-varying correlations during the

sample period indicate that investors frequently change their portfolio position. Second, we document that total spillovers reach peaks during the 2008-2009 GFC and 2010-2012 ESDC, highlighting that economic and financial crises intensify the spillovers across global futures markets, which reduces the diversification opportunities for these markets. Third, we identify the FTSE 100 as the most significant spillover contributor within our system, while the KOSPI 200 is the largest net receiver of shocks. Fourth, we depict the main results for a network of net pairwise connectedness, focusing on financial and economic events. We find that the net pairwise direction and intensity of network connectedness are sensitive to financial and economic events.

To conclude, from our study of network connectedness we are able to reveal information about direction and intensity of volatility spillovers across global futures markets. Moreover, this study explores the implications of connectedness' information on risk diversification, in the context of index and commodity portfolios involving different trading strategies or even across global futures markets.

Acknowledgment

The work reported in this paper was supported by the Korea Exchange in 2018.

References

Aielli, G.P., 2013. Dynamic conditional correlation: on properties and estimation. Journal of Business & Economic Statistics 31, 282–299.

Adrian, T., Brunnermeier, M., 2008. CoVaR. Staff Report 348. Federal Reserve Bank of New York.

An, S., Gao, X., Jiang, M., Sun, X., 2018. Multivariate financial time series in the light of complex network analysis. Physica A 503, 1241-1255.

Askari, M., Shirazi, H., Samani, K.A., 2018. Dynamics of financial crises in the world trade network. Physica A 501, 164-169.

Baillie, R.T., Bollerslev, T., Mikkelsen, H.O., 1996. Fractionally integrated generalized autoregressive conditional heteroskedasticity. Journal of Econometrics 74, 3–30.

Billio, M., Getmansky, M., Lo, A.W., Pelizzon, L., 2012. Econometric measures of connectedness and systemic risk in the finance and insurance sectors. Journal of Financial Economics, 104, 535-559.

Baumöhl, E., Kočenda, E., Lyócsa, Š., Výrost, T., 2018. Network of volatility spillovers among stock markets. Physica A 490, 1555-1574.

Cimini, R., 2015. Eurozone network “Connectedness” after fiscal year 2008. Financial Research Letters, 14, 160-166.

Dastkhan, H., Gharneh, N.S., 2018. How the ownership structures case epidemics in financial markets: A network-based simulation model. Physica A 492, 324-342.

Diebold, F.X., Yilmaz, K., 2016. Trans-Atlantic equity volatility connectedness: U.S. and European financial institutions, 2004-2014. Journal of Financial Econometrics, 14(1), 81-127.

Diebold, F.X., Yilmaz, K., 2014. On the network topology of variance decompositions: Measuring the connectedness of financial firms. Journal of Econometrics, 182, 119-134.

Diebold, F.X., Yilmaz, K., 2012. Better to give than to receive: Predictive directional measurement of volatility spillovers. International Journal of Forecasting, 28, 57-66.

Dimitrios, T., Charakopoulos, A., 2018. Visibility in the topology of complex networks. Physica A 505, 280-292.

Engle, R.F., Kelly, B., 2012. Dynamic equicorrelation. Journal of Business & Economic Statistics 30, 212–228.

Eom, C., G. Oh, W.-S. Jung, H. Jeong, and S. Kim, (2009). Topological properties of stock networks based on minimal spanning tree and random matrix theory in financial time series. Physica A, 388, 900-906.

Fernández-Rodríguez, F., Gómez-Puig, M., Sosvilla-Rivero, S., 2016. Using connectedness analysis to assess financial stress transmission in EMU sovereign bond market volatility. Journal of International Financial Markets, Institutions & Money, 41, 126-145.

Forbes, K.J., Rigobon, R., 2002. No contagion, only interdependence: Measuring stock market comovements. Journal of Finance 57, 2223-2261.

Greenwood-Nimmo, M., Nguyen, V.H., Rafferty, B., 2016. Risk and return spillovers among the G10 currencies. Journal of Financial Markets, 31, 43-62.

Kang, S.H., Mclver, R., Yoon, S.-M., Dynamic spillover effect among crude oil, precious metal, and agricultural commodity futures markets. Energy Economics, 62, 19-32.

Liu, X., An, H., Li, H., Chen, Z., Feng, S., Wen, S., 2017. Features of spillover networks in international financial markets: Evidence from the G20 countries. Physica A, 479, 265-278.

Majapa, M., Gossel, S.J., 2016. Topology of the South African stock market network across the 2008 financial crisis. Physica A 445, 35-47.

Majdoub, J., Mansour, W., 2014. Islamic equity market integration and volatility spillover between emerging and US stock markets. North American Journal of Economics and Finance, 29, 457-265.

Maghyereh, A.I., Awartani, B., Bouri, E., 2016. The directional volatility connectedness between crude oil and equity markets: New evidence from implied volatility indexes. Energy Economics, 57, 78-93.

Shahzad, S.J.H., Ferrer, R., Ballester, L., Umar, Z., 2017. Risk transmission between Islamic and conventional stock markets: A return and volatility spillover analysis. International Review of Financial Analysis, 52, 9-26.

Shahzad, S.J.H., Hernandez, J.A., Rehman, M., Al-Yahyaee, K.H., 2018a. A global network topology of stock markets: Transmitters and receivers of spillover effects. Physica A 492, 2136-2153.

Shahzad, S.J.H., Kayani, G.M., Raza, S.A., Shah, N., Al-Yahyee, K.H., 2018b. Connectedness between US industry level credit markets and determinants. Physica A 491, 874-886.

Xi, X., An, H., 2018. Research on energy stock market associated network structure based on financial indicators. Physica A 490, 1309-1323.

Xu, X.-J., Wang, K., Zhu, L., Zhang, L.-L., 2018. Efficient construction of threshold networks of stock markets. Physica A 509, 1080-1086.

Yu, J.-W., Xie, W.-J., Jiang, Z.-Q., 2018. Early warning model based on correlated networks in global crude oil markets. Physica A 490, 1335-1343.

Zhang, D., 2017. Oil shocks and stock markets revisited: Measuring connectedness from a global perspective. Energy Economics, 62, 323-333.

Zho, L., Wang, G.-J., Wang, M., Bao, W., Li, W., Eugene Stanley, H., 2018. Stock market as temporal network. Physica A 506. 1104-1112.